

Accessing Small Inner Working Angles with a Rotating Sub-aperture Nuller

E. Serabyn and B. Mennesson

Jet Propulsion Laboratory, California Institute of Technology, Pasadena, CA 91109, USA
email: gene.serabyn@jpl.nasa.gov

Abstract.

A new approach to high contrast observations near bright stars with a single-aperture telescope is discussed, which is based on the idea of a rotating separated-aperture nulling interferometer. The approach can be described as a rotating sub-aperture nuller, because it nulls two or more sub-apertures within a single telescope's pupil, and uses baseline rotation to modulate the signals from off-axis sources in a manner similar to that of potential space-based nulling interferometers. The sub-aperture beams can be combined in a number of ways, including a fiber nuller and a rotational shearing interferometer. Such a rotating nulling coronagraph has two great advantages. First, it can be used on a ground-based telescope to test signal reconstruction approaches pertinent to potential space-based nulling interferometers. Moreover, it also has the potential to enable ground-based coronagraphic observations of faint off-axis companions very close to bright stars.

Keywords. coronagraphy, nulling interferometry

1. Introduction

To enable the direct detection of faint companions very close to bright stars, the development of techniques such as coronagraphy on single-aperture telescopes, and nulling interferometry between multiple telescope apertures is required. However, nulling interferometry differs from normal long-baseline interferometry in one important respect - the need to maintain a null at fixed phase implies that the complex visibility of the source brightness distribution is in general not directly accessible. Instead, what is easily measurable is the flux transmitted by the instantaneous nulling fringe pattern, so that a direct Fourier inversion to the source plane is not possible. Instead, more indirect inversion techniques such as cross-correlation (Angel and Woolf 1997) are likely necessary.

While image reconstruction with a nulling interferometer may be more difficult, the nature of the measurement is clear. As the nulling interferometer rotates, the nulling fringe pattern centered on the star rotates with it (Bracewell 1978). As the fringe pattern rotates, the fringes sweep across the position of the off-axis companion (Fig. 1), modulating its transmitted flux. For larger off-axis source offsets, in general more fringes cross the planet's position, and so higher harmonics are generated in the detected signal. The harmonic content of the signal thus determines the companion's angular offset from the nulled star, while the azimuth of the flux maxima determine its azimuth.

Given the novelty of this rotating long-baseline nulling approach, which is under consideration for space-based nulling interferometers, and given the ambiguity inherent in image reconstruction without full complex visibility data, it would clearly be very valuable to have a means of demonstrating both the viability of the approach, as well as the robustness of signal reconstruction algorithms, by means of a ground-based experiment prior to launch. These considerations led us the possibility of implementing a rotating

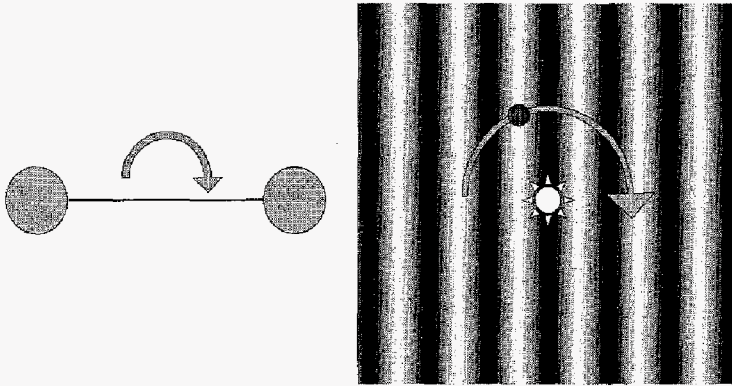


Figure 1. Schematic of a rotating long-baseline nuller and the accompanying fringe pattern. Destructive interference is maintained at the stellar position as the baseline and fringe pattern rotate. The companion's flux is modulated as the transmission fringes sweep past.

nuller on a single ground-based telescope, by establishing a baseline between separated subapertures. In the course of these considerations, it became clear that such an experiment would also provide unique coronagraphic capabilities. In the following, we describe the possible implementations and potential advantages of this idea.

2. The Idea

Whatever optical implementation is chosen to define the sub-apertures within the telescope pupil, and to combine the individual beams into a nulling baseline or baselines, it will be desirable to maximize the subaperture areas and the spectral bandwidth, in order to maximize the signal to noise (SNR) ratio. It will also be desirable to maximize the baseline length, in order to maximize the angular resolution. However, one could in principle trade off subaperture diameter against subaperture number, in order to maintain a high SNR, and to increase the field-of-view (FOV), as discussed below. Of course, at the outset it will be very important to select an optical implementation which is both simple and amenable to pathlength control, and so here we concentrate mostly on the single baseline case.

Although in principle a number of different beam-combination schemes can be used to combine and null the light from two subapertures lying within a given telescope pupil, including linear and rotational shearing interferometers, perhaps the simplest approach is the fiber nuller. This beam combiner (Fig. 2) is based on the injection of a number of beams into a common single-mode fiber in the focal plane (Wallner *et al.* 2004). Deep nulling of monochromatic light to close to the 10^{-6} level has now been demonstrated with a fiber nuller at JPL (Haguenaer and Serabyn 2005). For more broadband nulling, an achromatic phase shifter to introduce π radian (or other) phase shifts between the beams is needed. In principle, solutions for glass dispersion correctors do exist. However, a fiber nuller beam combiner has not yet been used for on-sky observations. In addition, with only two beams, the combiner injection efficiency is low (Fig. 3).

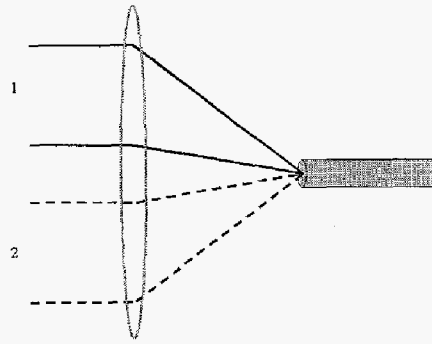


Figure 2. Schematic of a fiber nuller. Two spatially-separated beams are focused by a common optic onto a common single mode fiber. A relative phase shift of π radians is applied upstream.

In the simplest possible optical configuration with a fiber nuller beam combiner, a rotating dual-aperture mask in the pupil plane would select the two beams to be combined at the fiber tip (Fig. 4a). In this approach, the achromatic phase shifter would either need to rotate with the subaperture mask, or it would be necessary to accept a large dead zone in rotation angle, as the subapertures transition across the phase step. Neither of these solutions is ideal. These disadvantages can be obviated if a pupil rotator is inserted into the beam train, in which case a fixed dual-subaperture mask can be used to define the subapertures (Fig. 4b). On the other hand, such an approach brings with it the need for a very planar pupil rotation.

As mentioned, with a two-beam fiber nuller, the injection efficiency is low (Fig. 3). The efficiency loss inherent in the dual-beam fiber nulling approach can be recovered by instead using a more classical beamsplitter-based beamcombiner. In this regard a rotational shearing interferometer (RSI) also provides several additional advantages (Fig 4c). First, since RSIs combine two pupil images rotated by 180 degrees, all baselines centered on the pupil are generated simultaneously. Second, any given baseline can then be selected by means of a single off-center sub-aperture. Third, the light in this single sub-aperture can be focused with high efficiency into a fiber. Fourth, each baseline is duplicated on the opposite side of the center in the recombined pupil. This duplicate baseline can be made use of for e.g., a second waveband, or phase measurement and control. Finally, a number of baselines can be accessed simultaneously by means of different off-axis subapertures feeding different fibers, thus achieving pupil efficiencies approaching unity. Of course, all of these baselines can be rotated simultaneously by means of a common pupil rotator ahead of the RSI. Thus, inclusion of an RSI brings a number of significant advantages, and provides perhaps the best overall approach, although it is also the most complex of the approaches listed in Fig. 4

3. Performance

How well might such a rotating subaperture nuller perform? Other than sensitivity, the two main areas of interest are the achievable contrast, and the inner working distance (IWD), i.e., the smallest angular offset at which a companion can be detected. The IWD is given by $IWD = \frac{\alpha\lambda}{2b}$, where λ is the wavelength, b the baseline length, and α a constant of order unity. Note that $\frac{\lambda}{2b}$ is the angular offset to the first constructive fringe peak. There is a certain degree of freedom in specifying α , and different potential choices range

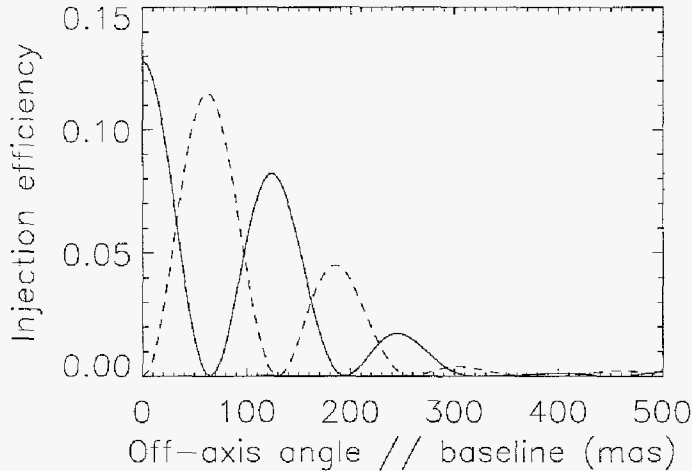


Figure 3. Injection efficiency of a pair of off-center beams into a single mode fiber for the case of 1.5 m subapertures and a 3.5 m baseline. For this plot, the off-axis companion is in the direction parallel to the baseline. Smaller subapertures would access additional fringes further off-axis.

from e.g., the fringe half-power point ($\alpha = \frac{1}{2}$), to just under unity ($\alpha \approx 0.85$) if the centralmost region where positional information is lost is to be avoided.

Since the maximum baseline length available is $D - s$, where D is the telescope diameter and s the subaperture diameter, we have $IWD = \frac{\alpha\lambda}{2(D-s)}$. For e.g., $s = D/3$, we then have $IWD = \frac{3\alpha}{4} \frac{\lambda}{D}$. Thus, independent of the exact value of α , this approach provides an IWD significantly smaller ($\sim \frac{1}{2} \frac{\lambda}{D}$) than that of a classical coronagraph (several λ/D).

The FOV is set by the width of the subaperture beam coupling to the single mode fiber. In the RSI combiner case, we have $FOV \approx \lambda/s$, so that smaller subapertures come with an increased FOV. In general, $FOV/IWD = \frac{2(D-s)}{s\alpha}$. In the case of $s = D/3$ discussed earlier, $FOV \approx 3\lambda/D$, and $FOV/IWD = 4/\alpha$. The accessible angles are thus somewhat restricted, but they cover a range otherwise inaccessible.

The attainable stellar null depth, N (the ratio of fluxes in the destructive and constructive states), will be limited mainly by the phase offset, ϕ between the two subaperture beams being combined, and is given by $N = (\phi/2)^2$. The expected null depth can therefore be estimated from the root-mean-square phase across the aperture, obtainable from the Strehl ratio, S , by means of the relation $S = 1 - \phi^2$, which applies for small ϕ . Thus, $N \approx (1 - S)/4$. For a typical current-generation adaptive optics (AO) system, with $S \approx 0.6$, and $\phi \approx 200$ nm, the rms null is then expected to be of order 0.1. However, due to path length fluctuations, the null depth will upon occasion reach much deeper levels, making the lower envelope of the null depth fluctuations the quantity of interest.

The detailed performance expected with a basic subaperture nuller behind a current-generation AO system is shown in Figure 5. These simulations of instantaneous null depth reproduce the expected 0.1 rms null level (the upper envelope of the traces), and also show that even without further phase correction, off-axis sources can be detected by means of their effect on the lower envelope of the null depth fluctuations. At each rotation angle of the baseline, one simply measures the null over a long enough time interval for the lower envelope of the null depth fluctuations to show the expected variations.

However, with the next generation of AO systems, with Strehl ratios of order 0.95 and $\phi \approx 75$ nm, the uncorrected rms null (or the upper envelope of the curves in Figure 5) can be expected to be as low 0.01, thus improving expected performance by an order of

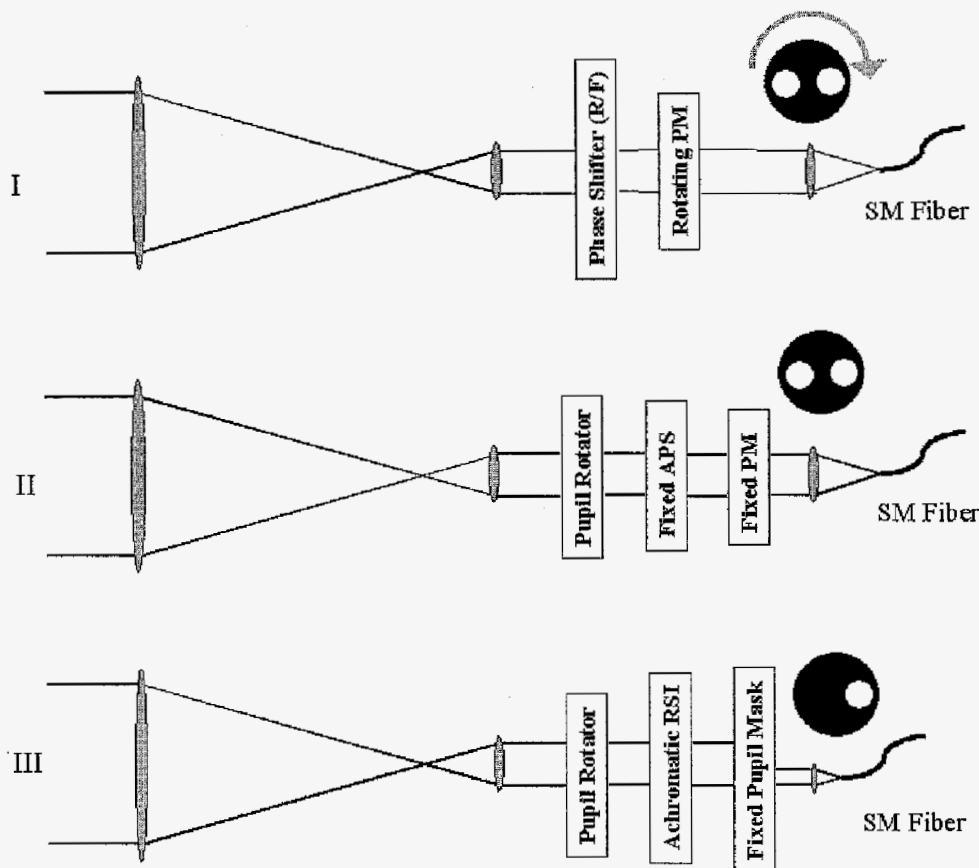


Figure 4. Three potential layouts for a rotating nulling coronagraph. R/F means “rotating or fixed”, PM is short for “pupil mask”, APS is “achromatic phase shifter”, and RSI is “rotational shearing interferometer.” In version III, only a single subaperture in the PM is necessary, although more subapertures can be used to increase efficiency or to lay out different nulling configurations, if each subaperture/baseline is coupled to its own fiber through its own lens.

magnitude. Note that such an AO performance level is actually already available today on the Palomar off-axis subaperture reimager (Serabyn *et al.*, these proc., Haguenaer *et al.* 2005), and can be made use of if a rotating nuller were to follow such a subaperture reimager.

However, a more active improvement is also possible. Since the null depth is limited by the phase fluctuations between the two large subapertures, an accurate measurement of this phase difference, and correction for it, can directly improve the null stability. Because of the large size of the subapertures, the SNR of such a measurement will be high. Thus, with a second, post-AO, layer of phase correction, significant improvement in the null depth stability can be achieved.

4. Conclusions

A rotating single-baseline sub-aperture nuller coupled to a single-aperture ground-based telescope can be used both to test the rotating nulling interferometer approach

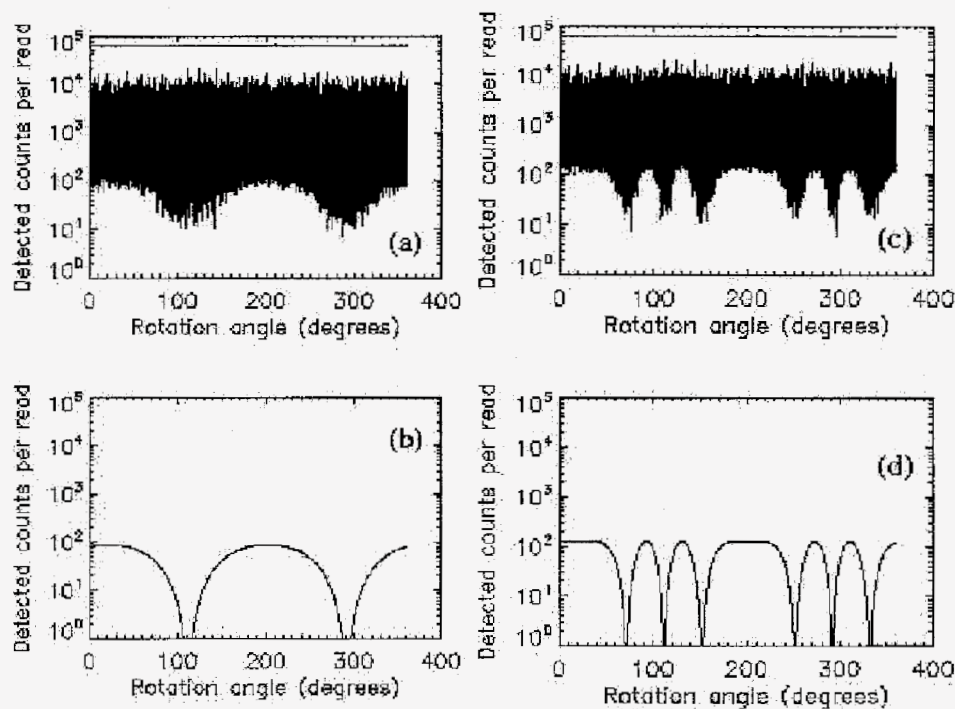


Figure 5. Expected performance of a rotating sub-aperture nuller on the Palomar 200 inch telescope in K band, without any phase stabilization beyond that provided by the Palomar AO system. Panels b and d show the expected null depths vs. rotation angle for a pair of binaries of contrast 500, for separations of 40 mas and 200 mas, respectively. Panels a and c show simulations of the null depths measured. The constructive state is shown by the horizontal lines in the panels. The bottom of the null depth fluctuation envelopes follow the theoretical curves. Phase stabilization between the subapertures will improve the performance.

being considered for space-based interferometers by NASA and ESA, and also to generate a coronagraph with a small inner working angle. This type of nulling coronagraph can be implemented in a number of ways, from a simple rotating pupil mask with a fiber combiner, to a more complex but more capable system which includes an RSI as well as a pupil rotator. Likewise, a number of possible subaperture configurations are possible, allowing for either an increase in efficiency, for phase correction, or for the testing of different potential pupil configurations.

Acknowledgements

This work was carried out at the Jet Propulsion Laboratory, California Institute of Technology, under contract with the National Aeronautics and Space Administration

References

- Angel, J.R.P. & Woolf, N.J. 1997, *ApJ* 475, 373
- Bracewell, R.N. 1978, *Nature* 274, 780
- Haguenauer, P. & Serabyn, E. 2005, *Applied Optics* in press
- Haguenauer, P. *et al.* 2005, *Proc. SPIE* 5905, 59050S-1
- Wallner, O., Perdigues Armengol, J.M., Karlsson, A.L. 2004, *Proc. SPIE* 5491, 798